University of Groningen

Laser Spectroscopy of Trapped Ra+ Ion

Versolato, Oscar Oreste

IMPORTANT NOTE: You are advised to consult the publisher's version (publisher's PDF) if you wish to cite from it. Please check the document version below.

Document Version
Publisher's PDF, also known as Version of record

Publication date:
2011

Link to publication in University of Groningen/UMCG research database

Citation for published version (APA):
Versolato, O. O. (2011). *Laser Spectroscopy of Trapped Ra+ Ion: Towards a single ion optical clock*. [Thesis fully internal (DIV), University of Groningen]. s.n.

Copyright
Other than for strictly personal use, it is not permitted to download or to forward/distribute the text or part of it without the consent of the author(s) and/or copyright holder(s), unless the work is under an open content license (like Creative Commons).

The publication may also be distributed here under the terms of Article 25fa of the Dutch Copyright Act, indicated by the "Taverne" license. More information can be found on the University of Groningen website: https://www.rug.nl/library/open-access/self-archiving-pure/taverne-amendment.

Take-down policy
If you believe that this document breaches copyright please contact us providing details, and we will remove access to the work immediately and investigate your claim.

Downloaded from the University of Groningen/UMCG research database (Pure): http://www.rug.nl/research/portal. For technical reasons the number of authors shown on this cover page is limited to 10 maximum.

Download date: 05-05-2023

CHAPTER 4

Laser Spectroscopy of Trapped Short-Lived Ra^+ Ions

Laser spectroscopy experiments were performed with on-line produced short-lived $^{212,213,214}Ra^+$ *ions as an important step towards an atomic parity violation experiment in one single trapped* Ra^+ *ion*[1]*. The isotope shift of the* $6d\,^2D_{3/2}$ - $7p\,^2P_{1/2}$ *and* $6d\,^2D_{3/2}$ - $7p\,^2P_{3/2}$ *transitions and the hyperfine structure constant of the* $7p\,^2P_{1/2}$ *and* $6d\,^2D_{3/2}$ *states in* $^{213}Ra^+$ *were measured. These values provide a benchmark for the required atomic theory. A lower limit of* 232(4) *ms for the lifetime of the metastable* $6d\,^2D_{5/2}$ *state was measured by optical shelving.*

4.1 Motivation

The radium ion Ra^+ is a promising candidate for an atomic parity violation (APV) experiment with one single trapped ion [29–32]. APV experiments [10, 34–37, 40] are sensitive probes of the electroweak interaction at low energy. APV is due to the exchange of the Z^0 boson between the electrons and the quarks in the atomic nucleus. Its size depends on the mixing angle of the photon and the Z^0 boson, which is a fundamental parameter of the electroweak theory. The APV signal is strongly enhanced in heavy atoms [40] and it is measurable by exciting suppressed

[1] Results in this Chapter are the basis of [82–84]. Here some additional information is provided.

(M1, E2) transitions [85]. The predicted enhancement in Ra^+ is about 50 times larger than in Cs atoms [32, 41, 42], for which the most accurate measurement has been performed [34, 35, 38]. However, laser spectroscopy on trapped Ra^+ ions has not been performed yet, and certain spectroscopic information, needed to test the required atomic many-body theory, is lacking [32]. For instance, the lifetimes of the $6d\,^2D_{3/2}$ and $6d\,^2D_{5/2}$ states, which are important quantities for a single-ion APV experiment, have not been measured yet. These states are also relevant for a potential Ra^+ optical clock [44, 70, 86].

4.2 Experimental Status

Up to now, accurate experimental information on the optical spectrum of Ra^+ (see Fig. 4.1) was only available from measurements at the ISOLDE facility at CERN, where the isotope shift (IS) and hyperfine structure (HFS) of the $7s\,^2S_{1/2}$, $7p\,^2P_{1/2}$, and $7p\,^2P_{3/2}$ states were obtained by collinear spectroscopy over a large range of isotopes [25, 64]. The only absolute measurement of the relevant wavelengths dates back to arc emission spectroscopy performed on $^{226}Ra^+$ in 1933 [28]. We present here the results of on-line excited-state laser spectroscopy experiments of trapped, short-lived $^{212,213,214}Ra^+$ ions, obtained at the TRIμP facility [76] of the KVI in Groningen. IS and HFS measurements were performed to constrain the atomic theory: HFS is a sensitive probe of the atomic wave functions in the nucleus [87], the accuracy of which is important for APV and clock experiments, while experiments on different isotopes serve to cancel remaining uncertainties in the atomic theory [32].

4.2.1 Experimental Setup

The experimental setup was discussed in detail in Chapter 3. For completeness, the key points are repeated below.

Production

Radium isotopes were produced in inverse kinematics by bombarding a 4 mg/cm^2 diamond-like carbon foil with an 8.5 MeV/nucleon ^{206}Pb beam with typically 3×10^{10} particles/s from the AGOR cyclotron, and emerged from the fusion-evaporation reactions $^{206}Pb + {}^{12}C \rightarrow {}^{218-x}Ra$, in which x neutrons were liberated. The isotopes ^{212}Ra, ^{213}Ra, and ^{214}Ra were separated from the primary beam and fission products in the magnetic separator [75]. They were stopped and re-ionized to Ra^+ in a Thermal Ionizer (TI) [77] with a transmission efficiency of up to 9%. Rates of 800 $^{212}Ra^+$/s, 2600 $^{213}Ra^+$/s, and 1000 $^{214}Ra^+$/s were extracted as an ion beam with an energy of 2.8 keV. The Ra^+ isotopes were passed through a

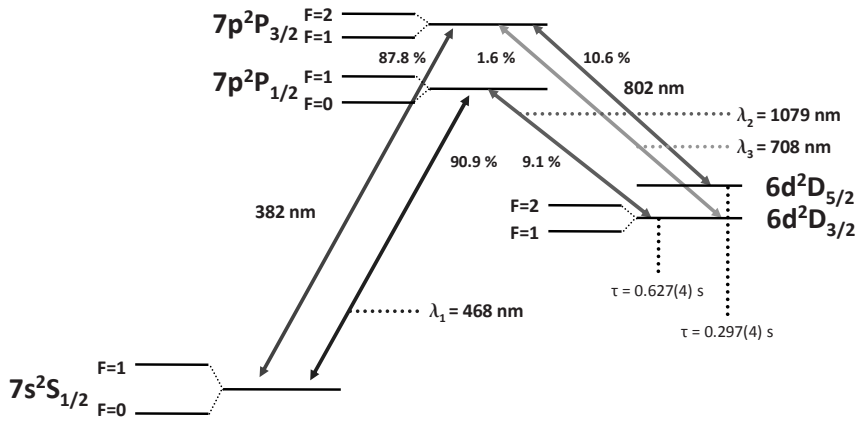

Figure 4.1: $^{213}Ra^{+}$ level scheme. The wavelengths are from Ref. [28]. Branching ratios and lifetimes are calculated in Ref. [70].

Wien Filter (which eliminated contaminants from the TI), and electrostatically decelerated upon injection in a (N_2 or Ne) gas-filled Radio Frequency Quadrupole (RFQ) cooler [78], operated at a frequency of 500 kHz with a peak-to-peak RF voltage of $V_{\mathrm{RF}} = 380$ V applied between neighboring rods; the opposite half-moon-shaped electrodes, 10 mm in length, had a tip distance of 5 mm. For on-line optical spectroscopy, the ions were trapped at the end of the RFQ by suitable axial potentials, *i.e.* a Paul trap (see Fig. 4.2). The effective potential depth was 13 V while the axial potential depth was 10 V. Typically 10^3 $^{212}Ra^{+}$, 10^4 $^{213}Ra^{+}$,

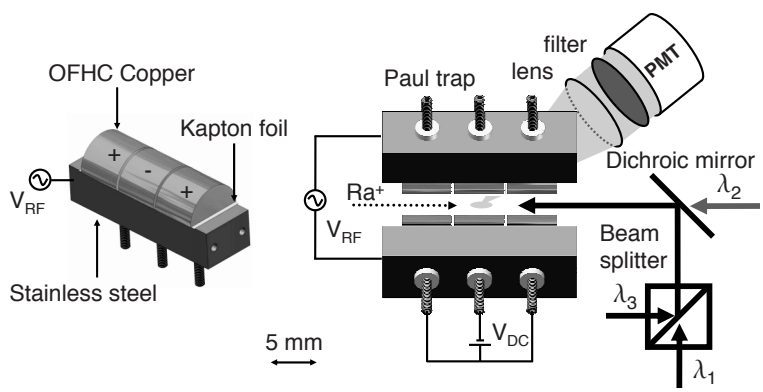

Figure 4.2: Schematic overview of the experimental setup behind the RFQ cooler.

and 10^2 $^{214}Ra^+$ ions could be stored. The storage time was of order 100 s at a residual gas pressure of 10^{-8} mbar (the lifetimes for radioactive decay are 13 s, 164 s, and 2.5 s for ^{212}Ra, ^{213}Ra, and ^{214}Ra, respectively). A N_2 or Ne buffer gas was used to aid effective catching and trapping of the radioactive particles from the beam in the RFQ. This gas dissipated the large (eV) energies of the ion beam, compressed the trapped cloud, and also enhanced the storage time. The buffer gas influenced the level lifetimes of the ions because of optical quenching and (hyper)fine-structure mixing of the metastable states. It was expected that Ne had the smallest influence on the level lifetimes [58].

Laser Setup

Home-built Extended Cavity Diode Lasers (ECDLs) were used to drive the optical transitions (see Fig. 4.1). Light to drive the $7s\,^2S_{1/2}$ - $7p\,^2P_{1/2}$ transition at wavelength $\lambda_1 = 468$ nm came from NDHA210APAE1 laser diodes from Nichia (see Fig. 3.11); the $6d\,^2D_{3/2}$ - $7p\,^2P_{1/2}$ transition at wavelength $\lambda_2 = 1079$ nm was driven with light from a LD-1080-0075-1 diode from Toptica; the $6d\,^2D_{3/2}$ - $7p\,^2P_{3/2}$ line at wavelength $\lambda_3 = 708$ nm was excited with light from a HL7001MG diode from Opnext. The laser light was delivered to the ion trap with single-mode optical fibers. The beams were overlapped with polarizing beam splitters and a dichroic mirror and sent axially through the trap to minimize scattered light. They were focused to 1 mm diameter at the trap location. Typical laser beam powers P at the trap center were $P(\lambda_1) = 300\ \mu$W, $P(\lambda_2) = 600\ \mu$W, and $P(\lambda_3) = 150\ \mu$W. The wavelengths were monitored with two HighFinesse Ångstrom WS6 VIS and IR wavelength meters. Absolute frequency calibration for light at λ_1 was provided by an absorption line in Te_2 through linear absorption in a Te_2 glass cell at 450 K. Light at λ_3 was calibrated by linear absorption at the P(146)(2-8) resonance in I_2 in a cell at 500 K. Since for wavelength λ_2 no similar reference was available, it was determined with the IR wavelength meter. The IR wavelength meter was continuously cross-referenced with a cavity of finesse 100 and free spectral range (FSR) 5 GHz. The transitions in Ra^+ were detected through fluorescence light from the $7s\,^2S_{1/2}$ - $7p\,^2P_{1/2}$ transition at wavelength λ_1. Because of the 10% branching into the metastable $6d\,^2D_{3/2}$ state, this fluorescence was only observed when both the $7s\,^2S_{1/2}$ - $7p\,^2P_{1/2}$ and $6d\,^2D_{3/2}$ - $7p\,^2P_{1/2}$ transitions were resonantly excited. The fluorescence light was imaged with a single lens of focal length $f = 30$ mm inside the vacuum through a low-pass filter with 80% transmission for wavelengths shorter than 500 nm (Thorlabs FES0500) onto the photocathode of a photomultiplier (Hamamatsu R7449). The collection solid angle was 0.4 sr.

4.3 Results

4.3.1 Detection of the $7s\,^2\mathrm{S}_{1/2}$ - $7p\,^2\mathrm{P}_{1/2}$ Transition

The absolute wavelength of the $7s\,^2\mathrm{S}_{1/2}$ - $7p\,^2\mathrm{P}_{1/2}$ transition in $^{212-214}\mathrm{Ra}^+$ can be derived by scaling the measurements performed on $^{226}\mathrm{Ra}^+$ [28] by the more accurate isotope shifts established by the ISOLDE collaboration at CERN [64]. However, a large uncertainty of several GHz remained due to the uncertainties given in Ref. [28]. Here, the results of the accurate determination of the absolute frequency of the $7s\,^2\mathrm{S}_{1/2}$ - $7p\,^2\mathrm{P}_{1/2}$ transition in $^{212}\mathrm{Ra}^+$ are presented. This absolute frequency was determined by scanning the frequency of the laser light at λ_1 over the $7s\,^2\mathrm{S}_{1/2}$ - $7p\,^2\mathrm{P}_{1/2}$ resonance. Nitrogen buffer gas at relatively high pressures of typically 2×10^{-3} mbar was used to sufficiently reduce the lifetime of the metastable $6d\,^2\mathrm{D}_{3/2}$ level by means of optical quenching. Therefore, no repump laser light at wavelength λ_2 was necessary. The frequency of the laser light at λ_1 was monitored with a HighFinesse Ångstrom WS6 VIS wavelength meter. The absorption line in Te_2 at frequency 640, 146, 536(70) MHz (no. 178 in Ref. [81]) provided absolute frequency calibration. The measured line shape is shown in Fig. 4.3. The frequency of the $7s\,^2\mathrm{S}_{1/2}$ - $7p\,^2\mathrm{P}_{1/2}$ transition in $^{212}\mathrm{Ra}^+$ was established at 640, 146, 714(158) MHz. This number is in good agreement with the value found for $^{226}\mathrm{Ra}^+$ in Ref. [28] when scaled with the isotope shift value from Ref. [64] to 640, 144, 943(1, 400) MHz. The wavelengths of the $7s\,^2\mathrm{S}_{1/2}$ - $7p\,^2\mathrm{P}_{1/2}$ transitions in the other isotopes were subsequently found by scaling the wavelength given above by the isotope shift values given in Ref. [64].

4.3.2 Hyperfine Structure

The wavelengths of the light from two diode lasers at λ_1 were kept close to the resonances $7s\,^2\mathrm{S}_{1/2}\,F{=}1$ - $7p\,^2\mathrm{P}_{1/2}\,F'{=}0$ and $7s\,^2\mathrm{S}_{1/2}\,F{=}0$ - $7p\,^2\mathrm{P}_{1/2}\,F'{=}1$ in order to study the HFS of the $6d\,^2\mathrm{D}_{3/2}$ - $7p\,^2\mathrm{P}_{1/2}$ transition in $^{213}\mathrm{Ra}^+$. The frequency of the laser light at λ_2 was scanned over the resonances. For this measurement N_2 buffer gas was used. Collisions admixed the two hyperfine levels of the $6d\,^2\mathrm{D}_{3/2}$ level, ensuring that no significant shelving to the metastable $6d\,^2\mathrm{D}_{3/2}\,F{=}1$ ($F{=}2$) state occurred when the $6d\,^2\mathrm{D}_{3/2}\,F{=}2$ ($F{=}1$) state was depopulated by the resonant laser light at λ_2. The frequency was calibrated with the IR wavelength meter. The measured line shapes are shown in Fig. 4.4. The different Lorentzian linewidths are due to saturation effects related to various relaxation rates [66], here introduced by the buffer gas. The measured HFS splitting 4542(7) MHz for the $7p\,^2\mathrm{P}_{1/2}$ state is within 2 standard deviations of the value 4525(5) MHz obtained at ISOLDE [64]. For the $6d\,^2\mathrm{D}_{3/2}$ state the HFS splitting was measured as 1055(10) MHz; the extracted $7p\,^2\mathrm{P}_{1/2}$ and $6d\,^2\mathrm{D}_{3/2}$ HFS constants A are given in Table 4.1. The theoretical predictions [32, 42] are in good agreement with these values.

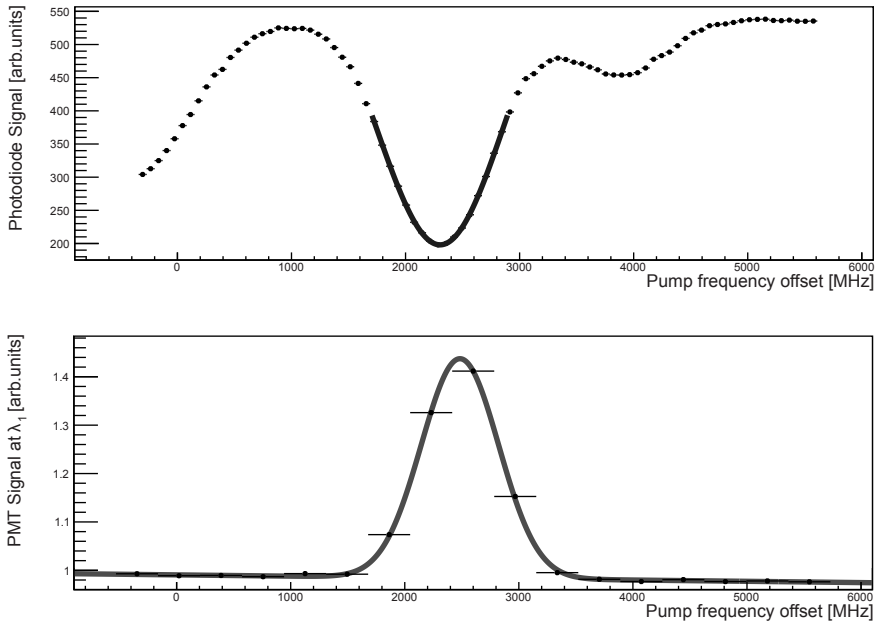

Figure 4.3: (a) Absorption spectrum of Te_2. The solid black line represents a Gaussian fit to the data. The width of the resonance is $565(15)_{\mathrm{stat}}$ MHz; it is centered at 2306(100) MHz. The reduced $\chi^2 = 1.1$ at 12 degrees of freedom (d.o.f.). (b) Line shape of the $7s\,^2\mathrm{S}_{1/2}$ - $7p\,^2\mathrm{P}_{1/2}$ transition in $^{212}\mathrm{Ra}^+$. The solid black line represents a Gaussian fit to the data. The width of the resonance is $339(5)_{\mathrm{stat}}$ MHz; it is centered at 2484(100) MHz. The reduced $\chi^2 = 0.8$ at 12 d.o.f. An additional uncertainty due to the calibration of the frequency axis was taken into account in the determination of the position of the resonances. The offset count rate of the PMT signal includes scattered photons from the pump laser light at λ_1 of order 10^4 counts/s as well as the dark count rate of the PMT (below 10^2 counts/s). The uncertainties of the PMT signal are based on the standard deviations of the bin contents as calculated using the TProfile class of CERN's ROOT code.

4.3.3 Isotope Shift of the $6d\,^2\mathrm{D}_{3/2}$ - $7p\,^2\mathrm{P}_{1/2}$ Transition

The IS for the $6d\,^2\mathrm{D}_{3/2}$ - $7p\,^2\mathrm{P}_{1/2}$ transition of Ra^+ was obtained with light from two lasers kept close to wavelength λ_1. One of these laser beams excited the $7s\,^2\mathrm{S}_{1/2}$ - $7p\,^2\mathrm{P}_{1/2}$ transition in $^{212}\mathrm{Ra}^+$, while the other one accessed either the same transition in $^{214}\mathrm{Ra}^+$ or the $7s\,^2\mathrm{S}_{1/2}\,F{=}1$ - $7p\,^2\mathrm{P}_{1/2}\,F'{=}0$ transition in $^{213}\mathrm{Ra}^+$. The frequency of the laser light at λ_2 was scanned over the $6d\,^2\mathrm{D}_{3/2}$ - $7p\,^2\mathrm{P}_{1/2}$ resonances of the isotopes under investigation (see Fig. 4.5). The IR wavelength

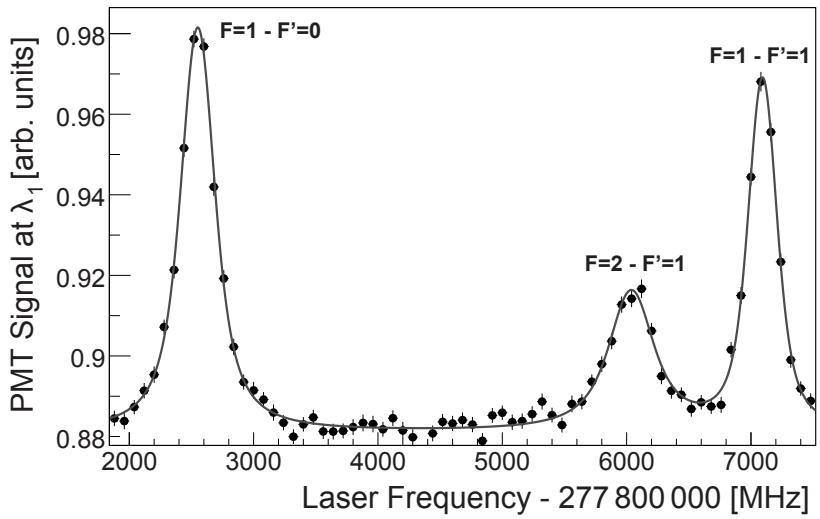

Figure 4.4: HFS of the $6d\,^2\mathrm{D}_{3/2}$ - $7p\,^2\mathrm{P}_{1/2}$ transition in $^{213}\mathrm{Ra}^+$. The solid line represents a fit of 3 Voigt profiles to the data. The Gaussian widths of the resonances are 181(20) MHz (FWHM). The Lorentzian widths (FWHM) are 245(20), 368(70), and 147(9) MHz (left to right). The different Lorentzian widths are due to saturation effects. The reduced $\chi^2 = 1.1$ at 62 d.o.f. The offset count rate of the PMT signal includes scattered photons from the pump laser light at λ_1 of order 10^4 counts/s as well as the dark count rate of the PMT (below 10^2 counts/s). The uncertainties of the PMT signal are based on the standard deviations of the bin contents as calculated using the TProfile class of CERN's ROOT code.

meter was used for frequency calibration. In order to minimize the influence of the buffer gas on the resonance line shape, only Ne was used. The measurements were performed at gas pressures 3×10^{-4}, 3×10^{-3}, and 2×10^{-2} mbar to study the influence of the buffer gas on the resonance line shapes. No significant effects on the measured IS were found. The resulting IS are summarized in Table 4.2.

4.3.4 Isotope Shift of the $6d\,^2\mathrm{D}_{3/2}$ - $7p\,^2\mathrm{P}_{3/2}$ Transition

For a determination of the IS of the $6d\,^2\mathrm{D}_{3/2}$ - $7p\,^2\mathrm{P}_{3/2}$ transition the lasers operating at λ_1 and λ_2 were kept close to resonance of a particular Ra^+ isotope. This created a fluorescence cycle. The frequency of the laser light at λ_3 was scanned over the resonances. Near resonance the ions were pumped to the $7p\,^2\mathrm{P}_{3/2}$ state, from which some 10% decayed to the $6d\,^2\mathrm{D}_{5/2}$ state (see Fig. 4.1). In this metastable

Table 4.1: HFS constants A [MHz] of the $7p\,^2P_{1/2}$ and $6d\,^2D_{3/2}$ states in $^{213}Ra^+$. The most recent theoretical values were converted to $^{213}Ra^+$ using the magnetic moment measured at ISOLDE [25]. The theoretical uncertainty is at the %-level.

	$7p\,^2P_{1/2}$	$6d\,^2D_{3/2}$
This work	4542(7)	528(5)
ISOLDE [64]	4525(5)	–
Theory [32]	4555	543
Theory [42]	4565	541

Table 4.2: IS [MHz] of the $6d\,^2D_{3/2}$ - $7p\,^2P_{1/2}$ and $6d\,^2D_{3/2}$ - $7p\,^2P_{3/2}$ transitions in Ra^+ isotope pairs. The measured values for the $6d\,^2D_{3/2}$ state and a value extracted from Refs. [25, 64] for the $7p\,^2P_{3/2}$ HFS were used to obtain the IS with respect to the center-of-mass of the resonances in $^{213}Ra^+$.

	$^{214}Ra^+ - ^{212}Ra^+$	$^{213}Ra^+ - ^{212}Ra^+$	$^{214}Ra^+ - ^{213}Ra^+$
$6d\,^2D_{3/2}$ - $7p\,^2P_{1/2}$	1032(5)	318(11)	714(12)
$6d\,^2D_{3/2}$ - $7p\,^2P_{3/2}$	701(50)	248(50)	453(34)

state the ions were shelved and did not participate in the fluorescence cycle. This caused a dip in the fluorescence signal, the position of which was calibrated against the P(146)(2-8) single-pass absorption resonance in molecular I_2 at $\nu_{\text{Iodine}} = 423\,433\,720$ MHz. The scan linearity was verified with a cavity of finesse 1200 and FSR 10 GHz. We found for the $6d\,^2D_{3/2}$ - $7p\,^2P_{3/2}$ transition $\nu_{212}=\nu_{\text{Iodine}} + 568(42)$ MHz for $^{212}Ra^+$ and $\nu_{214}=\nu_{\text{Iodine}} + 1269(23)$ MHz for $^{214}Ra^+$. For $^{213}Ra^+$ the fluorescence cycle was established by pumping on the $7s\,^2S_{1/2}\,F{=}1$ - $7p\,^2P_{1/2}\,F'{=}0$ transition and repumping on the $6d\,^2D_{3/2}\,F{=}1$ - $7p\,^2P_{1/2}\,F'{=}0$ transition. This left the $6d\,^2D_{3/2}\,F{=}2$ state largely depopulated. The frequency of the laser light at λ_3 was scanned over the resonances (see Fig. 4.6). The $6d\,^2D_{3/2}\,F{=}1$ - $7p\,^2P_{3/2}\,F'{=}1$ resonance is deformed by the close-lying $6d\,^2D_{3/2}\,F{=}2$ - $7p\,^2P_{3/2}\,F'{=}2$ transition as verified with a rate equation model. We use the $6d\,^2D_{3/2}\,F{=}2$ - $7p\,^2P_{3/2}\,F'{=}1$ resonance to determine the IS. The measurements were carried out at gas pressures 3×10^{-4}, 2×10^{-3}, and 2×10^{-2} mbar. The power of the laser beam at λ_3 was varied between 50 and 150 μW; no significant changes were found. We found $\nu_{213}=\nu_{\text{Iodine}} - 64(13)$ MHz. The measured isotope shifts are summarized in Table 4.2. The absolute frequency of the $6d\,^2D_{3/2}$ - $7p\,^2P_{3/2}$ transition in $^{212}Ra^+$ is 423 434 288(42) MHz. It had earlier been measured to be 423 437 660(570) MHz [28] for $^{226}Ra^+$, which yields an IS of 3.4(6) GHz.

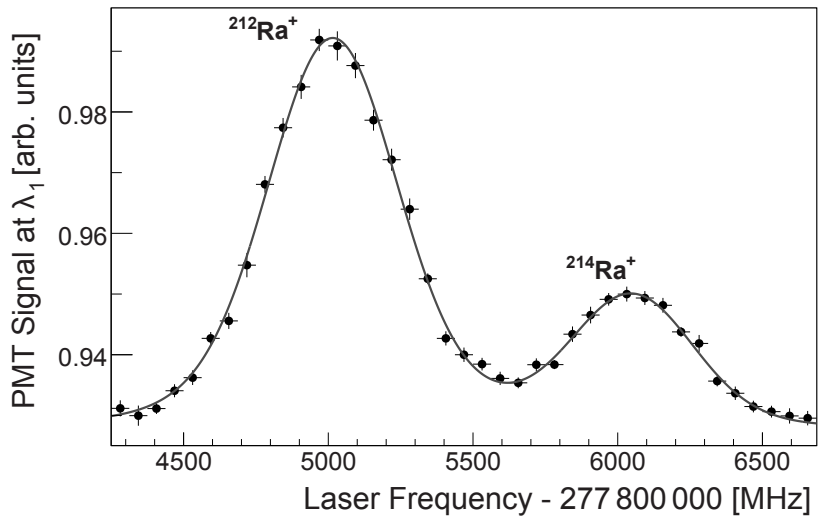

Figure 4.5: $6d\,^2\mathrm{D}_{3/2}$ - $7p\,^2\mathrm{P}_{1/2}$ resonances in $^{212}\mathrm{Ra}^+$ and $^{214}\mathrm{Ra}^+$. The solid line represents a fit of two Voigt profiles to the data. One parameter is used to fit the Gaussian widths of the two resonances, which yields a FWHM of 436(40) MHz. The Lorentzian widths (FWHM) are 201(50) MHz and 145(60) MHz (left to right). The reduced $\chi^2 = 0.92$ at 22 d.o.f.

4.3.5 Lifetime of the $6d\,^2\mathrm{D}_{5/2}$ Level

The demonstrated shelving to the $6d\,^2\mathrm{D}_{5/2}$ state by accessing the transition $6d\,^2\mathrm{D}_{3/2}$ - $7p\,^2\mathrm{P}_{3/2}$ also enables a measurement of the lifetime of this metastable state. The lasers at λ_1 and λ_2 were kept close to resonance in $^{212}\mathrm{Ra}^+$, while the laser light at λ_3 was pulsed with 170 ms on-periods and 670 ms off-periods by a mechanical chopper wheel. The laser light at λ_3 was kept on resonance to populate $6d\,^2\mathrm{D}_{5/2}$ via the $7p\,^2\mathrm{P}_{3/2}$ state. When the laser light at λ_3 was switched off, the $6d\,^2\mathrm{D}_{5/2}$ state depopulated and the ions re-entered the fluorescence cycle with a time constant equal to the lifetime of the $6d\,^2\mathrm{D}_{5/2}$ state (see Fig. 4.7). However, the neon buffer gas caused a reduction of the lifetime of the metastable state by quenching it to the ground state and by means of fine structure mixing between the $6d\,^2\mathrm{D}_{5/2}$ and $6d\,^2\mathrm{D}_{3/2}$ states. The latter effect causes the $6d\,^2\mathrm{D}_{5/2}$ state to be pumped out by the laser light at λ_2 *via* the $6d\,^2\mathrm{D}_{3/2}$ state. The fine structure mix rate is generally one or two orders of magnitude higher than the quench rate. To estimate these effects of the buffer gas, measurements were conducted at different gas pressures ranging from 10^{-2} to 10^{-5} mbar. No distinction between

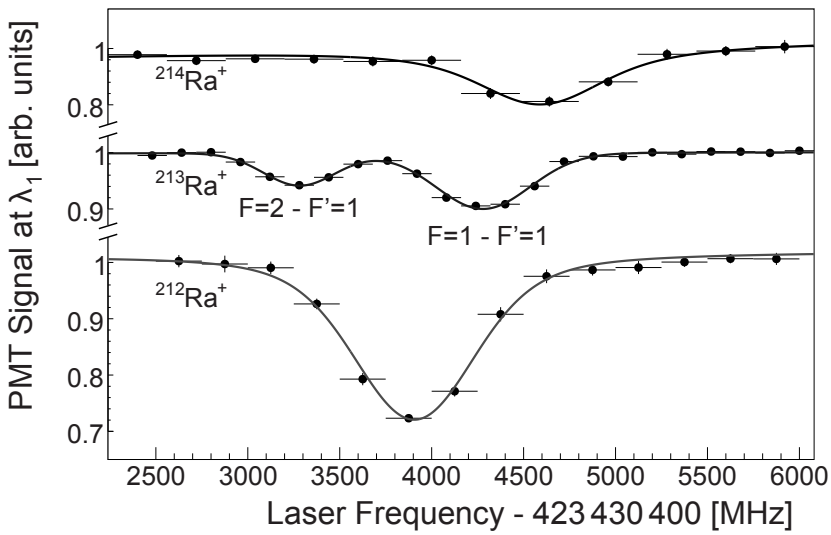

Figure 4.6: The $6d\,^2\mathrm{D}_{3/2}$ - $7p\,^2\mathrm{P}_{3/2}$ transitions. The solid lines represent fits of Voigt profiles to the data with reduced χ^2's of 0.81, 0.81, and 0.88 for $^{212}Ra^+$, $^{213}Ra^+$, and $^{214}Ra^+$, respectively, at 18, 26, and 17 d.o.f. The corresponding Gaussian and Lorentzian widths (FWHM) are 655(12) MHz and 243(10) MHz, respectively, for $^{212}Ra^+$, 363(30) and 144(23) MHz for the F=2 - F'=1 transition in $^{213}Ra^+$, and 451(270) MHz and 581(300) MHz for $^{214}Ra^+$. The different Gaussian widths are due to different neon buffer gas pressures. The different Lorentzian widths are caused by saturation effects which vary with gas pressure and laser power.

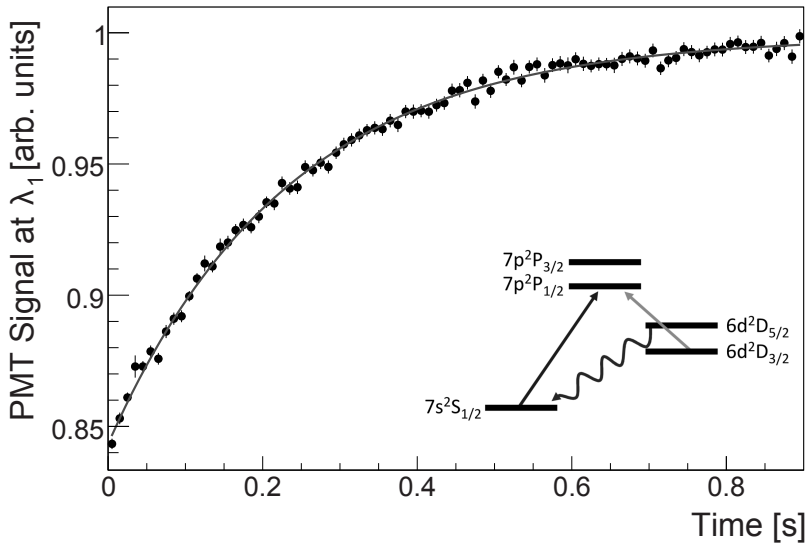

Figure 4.7: Lifetime measurements of the $^{212}\mathrm{Ra}^{+}$ $6d\,^2\mathrm{D}_{5/2}$ state at a neon buffer gas pressure of 4×10^{-5} mbar. The solid line represents a fit of an exponential function to the data. The fit yields a lifetime of 232(4) ms with a reduced $\chi^2 = 0.83$ at 87 degrees of freedom.

the effects of quenching and mixing could be made in these measurements: The dependence of the lifetime on these two effects is similar. The buffer gas was shown to have a strong influence on the optical lifetime (see Fig. 4.8). The gas pressure was monitored using a pirani-penning vacuum gauge (WRG D14701000 from BOC-Edwards) which was calibrated against a baratron. The uncertainties for the gas pressure readout are based (conservatively) on the difference between the baratron and the WRG readout. Assuming a linear dependence of the mixing rates on the gas pressure (see [57] and Chapter 2), the buffer gas pressure $\mathrm{P_{Ne}}$ dependence is given by

$$\tau_m = \left[\frac{1}{\tau_n} + \sum_i \alpha_i P_i \right]^{-1}, \tag{4.1}$$

where τ_m is the measured lifetime, τ_n is the natural radiative lifetime, α_i is the mixing or quenching rate per millibar of gas, for gas of type i of which P_i is the partial pressure. Residual partial pressures of other gases were measured below a few 10^{-7} mbar, and are neglected. The fit of Eq. 4.1 to the data yields $\tau_n = 231(4)$ ms, with a reduced $\chi^2 = 6.1$ at 2 degrees of freedom. The mixing or quenching

rate constant is found to be $\alpha_{Ne} = 562(105)$ mbar^{-1} s^{-1} or $2.2(4) \times 10^{-14}$ cm^3 s^{-1}. This rate is an order of magnitude lower than rates measured for other ions [58]. This can be explained by the exponential dependence of the mixing rates on the fine structure splitting [57] which is larger in radium at 1659 cm^{-1} than in the aforementioned other ions. For instance, it is 801 cm^{-1} for Ba^+ which indeed shows a higher mixing rate at $1.1(4) \times 10^{-13}$ cm^3 s^{-1} (see Chapter 2). The quenching rate is generally some two orders of magnitude smaller than the mixing rate [58]. The 5% confidence level corresponding to the fit indicates that the linear dependence breaks down over this large pressure range. No further detailed theory for this system is presently available to extrapolate the lifetime to zero pressure. A lower bound on the radiative lifetime of the $6d\,^2D_{5/2}$ state was found to be 232(4) ms; it corresponds to the lifetime measured at the lowest pressure of some 4×10^{-5} mbar (see Fig. 4.7). Corrections for the radioactive lifetime of ^{212}Ra and for the replacement time can be neglected. Theoretical predictions are 297(4) ms [70] and 303(4) ms [42]. Our experimental result is an important confirmation that the $6d\,^2D_{5/2}$ state is indeed long-lived. This is a necessary property in view of the long coherence times needed in APV and atomic clock experiments with a single trapped ion [29].

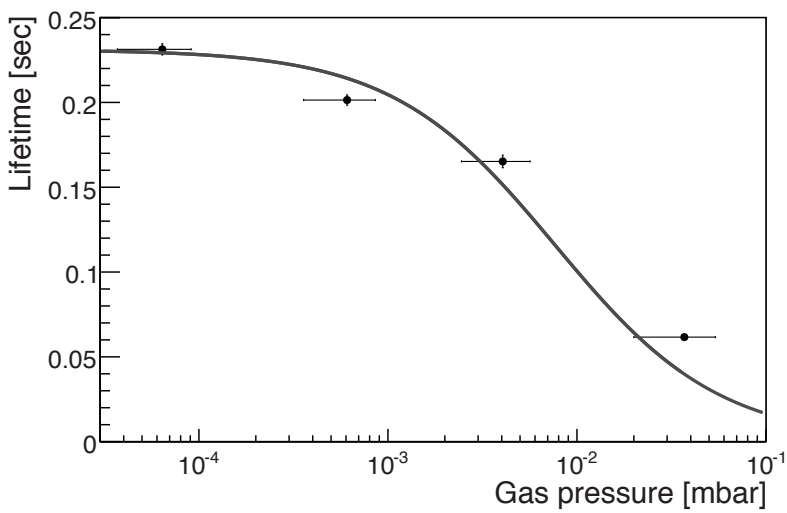

Figure 4.8: Lifetime of the Ra^+ $6d\,^2D_{5/2}$ state as a function of the neon buffer gas pressure. The solid line represents a fit of Eq. 4.1. The fit yields a $\chi^2 = 6.1$ at 2 degrees of freedom.

4.4 Discussion

Atomic parity violation (APV) experiments are sensitive probes of the electroweak interaction at low energy. Such experiments are competitive with and complementary to high-energy collider experiments. On-line excited-state laser spectroscopy was performed on short-lived trapped ions to measure indispensable experimental input for required atomic calculations. HFS measurements are suited to test wave functions at the origin, which is of particular importance for the estimation of the uncertainty of APV matrix elements [32, 70]. The data presented in this Chapter test theory at the percent level. Measurements of radiative lifetimes test atomic wave functions at larger distances. The lower bound of 232(4) ms established in this work is an important confirmation of the fundamental availability of long coherence times. IS measurements probe atomic theory and yield information about the size and shape of the atomic nucleus. Interpretation of these, and a more extended range of, IS measurements is published elsewhere [88]. These measurements test the atomic theory at the percent level. For the refinement of this test, Ra offers a chain of isotopes, where no measurements have been made and where theory is challenged to provide unbiased predictions.